NORDDESIGN CONFERENCE
REYKJAVIK, ICELAND, 12-14 AUGUST 2024

3D printing of Custom Hips for Orthopedic Training

Anton Wiberg[1], Hugo Blomqvist[1], Fredrik During[1], Rebecka Thim[1], Vilma Blixt[1], Fredrik Näslund[1], Rikard Gidlund[1], Fredrik Lundblad[1], Jörg Schilcher[2].

[1]Linköping University, Department of Management and Engineering
[2]Linköping University, Department of Biomedical and Clinical Sciences

Abstract: This research introduces a 3D printing process for creating anatomically precise hip models from CT scans for orthopedic training. It encompasses automated mesh cleaning and recommends specific materials and print settings for bone-like fidelity. Through structural assessments and expert collaboration, a user-friendly protocol is established, enhancing surgical training aids by closely mimicking real bone characteristics. This advancement holds significant promise for medical education, demonstrating the potential of 3D printing in improving surgical preparedness and patient care.

Keywords: Additive Manufacturing, 3D Printing, Design Automation, Healthcare Design

1 Introduction

Orthopaedic surgery a cornerstone of medical practice, shoulders the immense responsibility of addressing numerous of different kind of musculoskeletal disorders and injuries. Given the complexity of human anatomy and the vast variation across individuals, orthopaedists are often faced with intricate and patient-specific challenges (Soames and Palastanga, 2018). In recent times, technological advancements like CT scanning have been merged with software capabilities, enabling the creation of detailed digital three-dimensional models. These models are pivotal not only for diagnosis but also for procedural planning, ensuring a precision medicine approach to care (D'Urso et al., 1999; Marro et al., 2016).

One groundbreaking application of these digital models is their transformation into tangible assets using 3D printing. This technology brings numerous benefits: it offers hands-on models for surgical rehearsals, facilitates training for emerging orthopaedic surgeons, and promises a more personalized and safer patient care paradigm (Hoang et al., 2016; Rengier et al., 2010). However, the transition from a digital model to a 3D-printed replica is not without challenges. Current software, while adept at visualizing anatomy, may produce models with artifacts or other imperfections. This necessitates manual interventions to refine and optimize the digital blueprints for printing—a process that can be laborious (Michalski and Ross, 2014). Moreover, the choice of materials for 3D printing, particularly in orthopaedics, is critical. Although options like polyurethane foam models exist, they often fall short of capturing the specificity required for patient-centric applications (Liew et al., 2015).

This study advances the domain by introducing a streamlined approach for preparing 3D files for the creation of models that closely mimic bone in terms of material and internal architecture. We have developed a plugin for Blender (2018) that facilitates import and automatic rectification of 3D models derived from CT scans, often laden with artifacts such as holes and internal defects originating from the data conversion step after the CT scan which makes the model impossible to print. In addition, this research recommends specific materials and print settings to achieve bone-like consistency using conventional low cost and easily accessible material extrusion 3D printers and materials. The selection of materials and settings was determined through a structural assessment of various alternatives, executed in partnership with an expert orthopaedist. The result of this work is a user-friendly protocol that seamlessly transitions from an initial, imperfect 3D CT scan file to a 3D-printed hip model ready to be used for orthopaedic training.

This paper is divided into six sections where the introduction is followed by a presentation of background information about bone structures, 3D printing and some information about a pre-study on 3D printing of bone-like structures performed before this work started. Section 3 presents the evaluation of different materials and print settings performed within this work. In section 4, the procedure for cleaning meshes in Blender is presented. Section 5, Results, presents an overview of how the workflow can be used. The paper is finalised by a Discussion and conclusions section.

2 Background

2.1 Bone structures

Bones, the cornerstone of the human skeletal system, exhibit a diverse array of shapes and functionalities that can be broadly understood through their categorizations: long, short, flat, and irregular. For instance, long bones like the femur

and tibia are distinguished by an elongated shaft flanked by two ends, primarily providing support and aiding in movement. Short bones, such as the carpals and tarsals, exhibit a near equivalence in terms of length, width, and thickness, offering stability with a modicum of motion. On the other hand, the protective scapula and cranial bones fall under the flat bone category, which primarily safeguard underlying organs while serving as attachment points for muscles. Lastly, the irregular bones, which encompass vertebrae and select facial bones, present complex shapes that don't conform to the characteristics of the other categories (Saladin and Porth, 2010).

Delving deeper into the microscopic realm, the rich architectural intricacies of bones become evident. They are predominantly structured with an exterior cortical shell and an inner trabecular network. The dense cortical, or compact bone, enwraps all bones, pivotal in bearing the brunt of the mechanical load. Contrarily, the trabecular or cancellous bone forms the inner portions and exudes a spongy appearance. This spongy structure is particularly pronounced in the ends of long bones where they support the articular surface of the joint structure (Reilly and Currey, 1999). From a mechanical perspective, bones aren't mere static entities. These dynamic tissues possess unique mechanical properties that facilitate shock absorption, structural support, and movement facilitation. When exposed to external forces, bones demonstrate attributes such as elasticity, plasticity, and toughness. A noteworthy aspect of bones is their remodelling capability, where aged bone is systematically substituted with new bone. This ensures their sustained mechanical robustness and adaptability to variations in mechanical loadings (Rho et al., 1998; Robling et al., 2006). Figure 1 shows a basic illustration of a femur bone showing the difference between porous spongy bone and the dense compact bone.

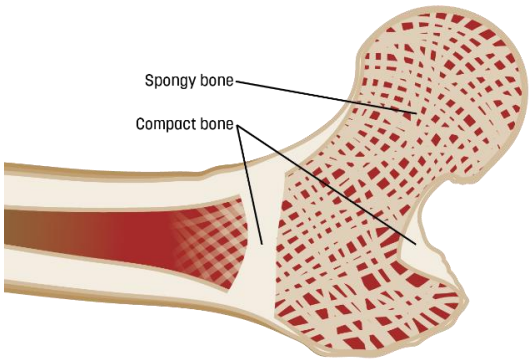

Figure 1. Illustration of the cross-section of a bone. Modified from Nefronus (2023).

2.2 3D printing

Additive manufacturing encompasses a number of different manufacturing processes but is often used synonymously with 3D printing. 3D printing is based on g-code, like other machines, to create a physical three-dimensional detail. Generally, details are built up from thin layers of material. One of the advantages of 3D printing is that it is cheaper for small production volumes than most other common manufacturing processes such as injection moulding and milling, which require expensive tools or machines (Davoudinejad, 2021; Kazmer, 2017). This means that 3D printing can be used for small-scale production and rapid prototyping. Fused Deposition Modelling (FDM) is a type of material extrusion where filament material is heated up and extruded onto a base plate, forming thin layers of the detail's cross-section (Kazmer, 2017). FDM machines generally operate by taking the material, in the form of a filament, which is placed on a spool and fed through tubes to the nozzle where the material is heated and extruded onto the base plate (Gibson et al., 2021). The nozzle moves in the X-Y direction over the base plate, building the detail's cross-section, with each new cross-section added in the Z-axis to create the final shape. After each layer, either the base plate moves downward or the nozzle moves upward, depending on the type of printer (O'Connell, 2018).

FDM enables the use of different kind of thermos polymers where the most common are PLA, ABS, PET, PETG, TPU, PC and Nylon (Treatstock, 2024). In addition, the materials can be mixed with additional materials such as carbon or glass fibre, wood, or other fibres or particles (Gibson et al., 2021). Furthermore, it allows manufacturing of two or more materials simultaneously. Each material has different properties, advantages, and disadvantages that affect the quality and durability of the printed objects. In the printing planning phase several settings can be changed, including layer height, nozzle size, number of contours, infill type, and density (Bardwell, 2023). These settings influence the resolution, strength, weight, and appearance of the printed objects. Therefore, finding the optimal combination of materials and settings for FDM printing requires careful experimentation and calibration based on the desired outcome (Ćwikla et al., 2017). Figure 2 shows how different settings can be applied to a geometry to achieve different printed results with the same geometry.

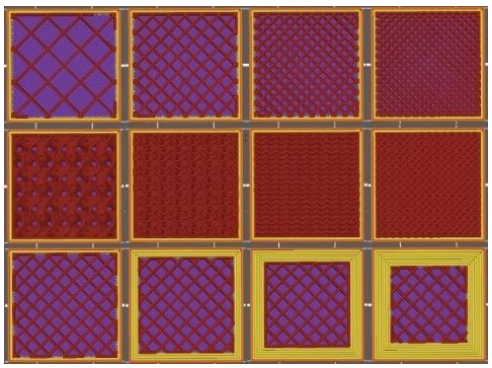

Figure 2. Variations in slicing settings. Top row and middle row showing variations in infill type (rectilinear and gyroid) with density from 20 to 80%. Bottom row showing variations in number of contours.

2.3 Pre-study

In response to the local orthopaedic community's request for an early evaluation of materials capable of mimicking bone-like structures, an unorganized testing was conducted using a FDM 3D printer. The aim was to rapidly assess various 3D printed materials to identify a potential candidate for manufacturing workshop materials for surgical training. How bone like a material is, was qualitatively judged based on the feeling when performing test orthopaedic surgeries and the look of cuttings during the procedures. Initial tests involved drilling into samples made from standard polymers like PLA and PET, both of which melted and failed to exhibit the desired behaviour under mechanical stress. However, PLA reinforced with wood fibres showed a marked improvement, not melting and more closely resembling the act of drilling into bone. Further evaluations considered different infill densities and patterns, with gyroid structures at 20-50% infill density emerging as the most bone-like in behaviour. This preliminary exploration suggests that while standard polymers are inadequate for such applications, composite materials like PLA with wood fibres, particularly when used with specific infill patterns, hold promise for creating bone-like structures in orthopaedic surgery.

3 Material evaluation

In the preliminary phase of the study, bolstered by a review of existing literature on materials, various material alternatives were swiftly identified. Two distinct methodologies for fabricating bone-like structures were selected for further exploration. The first method involves the use of FDM 3D printing technology, offering the flexibility to adjust both the material composition and printing parameters. The second method proposes the utilization of polyurethane foam, the current standard in commercially available models for surgical training. This innovative approach involves creating a 3D-printed outer shell that could be subsequently filled with foam, allowing for variable foam densities to closely mimic the structural properties of bone.

For the 3D-printed components, a selection of polymers infused with wood fibers was earmarked for detailed examination. Additionally, a specialized 3D printing material, Simubone, designed explicitly for simulating bone-like characteristics, was chosen for assessment. An overview of the 3D printing materials under consideration is provided in table 1, highlighting the diverse approaches being investigated to achieve the most bone-like properties in manufactured models.

Table 1. Overview of the 3D printing materials evaluated.

Material	Link	Comment
Polywood	https://www.3dprima.com/se/filament-resin/filament/wood/polymaker-polywood-pla_28624_10273 (accessed 2024-02-12)	PLA but manufactured with a foaming technique to behave like wood
Woodfill	https://colorfabb.com/woodfill (accessed 2024-02-12)	PLA/PHA with recycled wood fibers
Corkfill	https://colorfabb.com/corkfill (accessed 2024-02-12)	PLA/PHA with cork
Clas Ohlsson (CO)	https://www.clasohlson.com/se/Filament-PLA-tra-till-3D-skrivare,-Clas-Ohlson/p/38-9249 (accessed 2024-02-12)	PLA with wood fibers
Simubone	https://www.3dxtech.com/product/bone-modeling-filament/ (accessed 2024-02-12)	PLA with specialty additives to make it look and feel like bone

The evaluation of the materials was conducted in three distinct phases. In the initial phase, cubes crafted from each material, utilizing varied manufacturing settings, were rapidly assessed by a standard screwdriver and drill. The objective

of this phase was to facilitate a broad comparison across numerous manufacturing options. The second phase involved the production of full-scale hip models, albeit exclusively in one selected material. This stage aimed to determine the optimal wall thicknesses and to identify any potential challenges associated with fabricating complete hip implants. The evaluation process incorporated a comprehensive procedure that included milling with a basket drill and the insertion of implant screws, all overseen by a singular orthopedic surgeon specialist in hip revision surgery. During the tests the similarity to real bone was qualitatively judged based on the feeling when performing test orthopaedic surgeries and the look of cuttings during the procedures.

In the final phase, a workshop was convened with multiple orthopedic specialists participating. This culminated in a blind assessment of the final material candidate, where the experts completed a questionnaire to evaluate the material against various criteria, comparing its likeness to real bone. This structured approach allowed for an in-depth examination of the materials' suitability for orthopedic applications, leveraging expert opinions to ascertain the most promising candidate for bone-like structures.

Following the preliminary study, it was decided to fabricate all models using a gyroid infill pattern, with variations in infill density, number of wall layers, and nozzle sizes. All 3D printed models were produced using an Anycubic Kobra 2 FDM printer. The code for printing was meticulously prepared in the PrusaSlicer software, where the specific settings for each print were established.

3.1 Evaluation 1

In the initial experiment, various manufacturing settings were explored, including adjustments in 3D printing infill percentage, the number of wall layers, and nozzle size. Cubes with infill densities ranging from 20% to 50% (in increments of 5%) were utilized for the tests. An orthopedic surgeon conducted a rapid evaluation of these samples by drilling and inserting a screw into the test materials. The similarity of the drilling experience to that of conventional surgical procedures was qualitatively assessed and recorded for each sample. Due to material constraints, CO and Simubone were evaluated only in the most promising settings identified from the other materials at a subsequent time. Table 2 presents a ranking of the materials, focusing on infill percentages between 25-35%, as these were deemed to be the most promising among the tested cubes. Figure 3 provides a visual overview of the test samples.

Table 2. First evaluation of materials. Rating of impression of the similarity to bone, 1 not similar, 3 similar.

			Material				
Nozzle size (mm)	**Number of walls**	**Infill %**	**Polywood**	**Woodfill**	**Corkfill**	**CO**	**Simubone**
0.8	1	25, 30, 35	1	2	2		
0.8	2	25, 30, 35	2	3	2		
0.6	1	25, 30, 35	1	2	2		
0.6	2	25, 30, 35	2	3	2	3	3
0.6	3	25, 30		3		3	3
0.4	1	25, 30, 35	1	1	1		
0.4	2	25, 30, 35	2	2	2		

Figure 3. 3D printed samples evaluated in the first iteration.

The results indicated that CO and Simubone emerged as the most promising materials. Specifically, a wall thickness of 0.6 mm and the application of 2 layers were identified as optimal parameters for achieving the desired structural integrity and simulation quality. These findings underscore the potential of these materials in closely replicating the physical characteristics necessary for effective surgical training models and orthopedic applications.

Additionally, tests were conducted on polyethylene foam blocks of varying densities, sourced as pre-manufactured blocks without any walls or similar structural modifications. These blocks were evaluated for their tactile feel during manipulation, which was considered satisfactory. However, the tests revealed a significant drawback: the foam produced an excessive amount of dust during handling. This dustiness was deemed a critical issue, rendering the polyethylene foam blocks unsuitable for the intended application due to potential contamination and operational challenges in a surgical or clinical setting but also under workshop conditions.

3.1 Evaluation 2

In the subsequent phase of the investigation, a more comprehensive assessment was undertaken with the production and evaluation of full-scale hip bone models. The primary objective of this second iteration was to validate the optimal number of wall layers previously identified in the initial evaluation. This assessment was meticulously carried out by the same orthopedic surgeon who had conducted the first evaluation, employing a set of procedures that included drilling, screw driving, basket milling, and the intricate process of fitting a cup into the hip bone model.

To provide a detailed account of the experimental setup, Table 3 delineates the manufacturing parameters utilized for the two hip bone models subjected to evaluation, in addition to these the same settings as in evaluation 1 were used. Furthermore, Figure 4 illustrates a procedural example of the cup placement within the hip, offering visual insights into the methodology and the precision involved in the simulation of orthopedic surgical techniques. This stage of the research was instrumental in refining the understanding of the material and structural requirements necessary for creating anatomically accurate and functionally viable orthopedic models.

Table 3. Materials and manufacturing settings used during evaluation 2.

			Material
Nozzle size (mm)	**Number of walls**	**Infill %**	**CO**
0.6	2	30	3
0.6	3	30	2

Figure 4. The full procedure of placing a hip cup. Red circle shows the area where the bone is drilled out using a large circular mill. After reaching the appropriate roundness and size of hole, a metallic cup is hammered into place and fastened with screws along the blue arrows.

The outcomes of the evaluation revealed that there were notable issues with cracking along the layers (see figure 5), which appeared to be influenced by the direction of the milling relative to the orientation of the layers. Despite this challenge, the investigation confirmed that a wall thickness of 1.2mm, equivalent to two layers, emerged as the optimal specification. This finding underscores the importance of layer orientation and wall thickness in mitigating structural weaknesses, particularly in the context of simulating surgical procedures on 3D-printed orthopedic models. The identification of 1.2mm

as the most effective wall thickness provides a critical parameter for future manufacturing processes, aiming to enhance the durability and integrity of the models under the mechanical stresses encountered during surgical simulations.

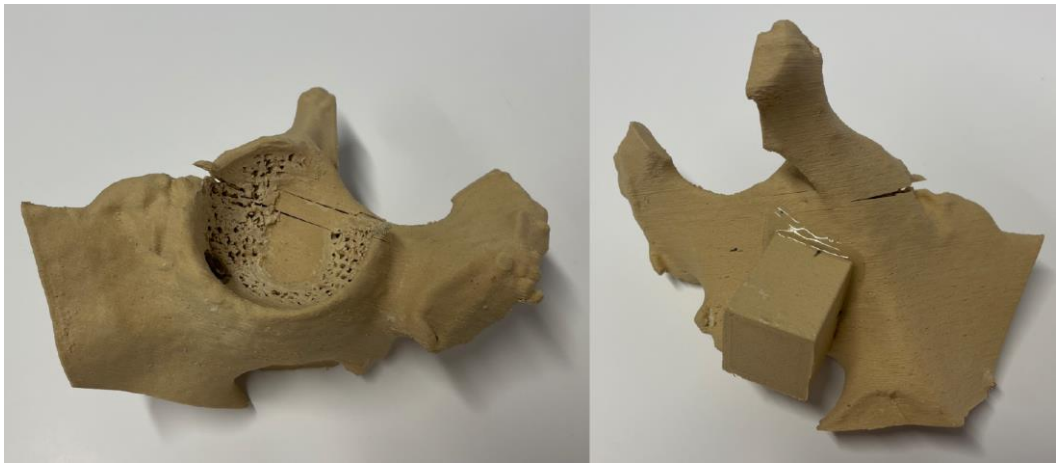

Figure 5. Problem with cracking occurred during evaluation 2.

3.3 Evaluation 3

A workshop was convened with five orthopedic specialists to conduct a comprehensive evaluation of full hip models, with a particular focus on optimizing the orientation to minimize cracking along the layers during impaction of the hip cup. The infill pattern selected for this purpose was the gyroid, known for its structural integrity and similarity to bone-like textures. A blind test methodology was employed to ensure unbiased feedback, with the evaluators anonymously submitting their observations from performing various procedures on the models, including basket milling, drilling, wrapping the cup, screw driving, and gauging. To systematically capture the evaluators' experiences, they were provided with a questionnaire designed to assess the models in terms of tactile, cosmetic, and mechanical realism, in addition to their usability for educational purposes. Each of these categories was to be rated on a scale from 1 to 10, with 10 being the highest possible score. A total of eight responses were collected through this process. The data gleaned from this workshop, including the specific types of models manufactured and their performance across the evaluated categories, is detailed in table 4. This structured approach to gathering expert feedback provided valuable insights into the potential of these 3D-printed hip models for surgical training, highlighting areas of strength and opportunities for further refinement to enhance their educational value.

Table 4. Models produced for the workshop.

Nozzle size (mm)	Number of walls	Infill %	Infill type	Number of Models	Material
0.6	2	30	Gyroid	2	CO
0.6	2	30	Gyroid	2	Simubone

Table 5 encapsulated the ratings from the questionnaire, covering a spectrum of criteria from first impressions to specific procedural outcomes and overall educational usability. Simubone received higher marks in texture (7 vs. 6.6) and color (8.5 vs. 7), suggesting a closer resemblance to natural bone aesthetics. In terms of procedural realism, both materials were rated closely in the milling process, indicating satisfactory performance. A significant divergence was however observed in drilling of the bone, where CO (8 and 8.3, respectively) markedly outperformed Simubone (5.5 in both categories), highlighting CO's superior performance in mimicking the resistance and feel of real bone during drilling. Other aspects such as gauging, chip formation, and the overall impression of the procedure showed relatively close scores between the two materials, with neither material demonstrating a decisive advantage. In the critical aspects of cup placement and stability, CO and Simubone were closely matched, though Simubone edged out slightly higher in cup stability (9.5 vs. 8), suggesting better long-term adherence in simulated surgical environments. Notably, both materials scored perfectly in usability for education (10), underscoring their potential in medical training contexts. The average scores, 7.6 for CO and 7.4 for Simubone, reflect a marginal preference for CO across the evaluated parameters, although both materials demonstrated considerable merits. These findings indicate that both CO and Simubone possess qualities that make them viable options for creating realistic and educationally valuable orthopedic surgical models, with specific strengths in different areas of application.

Table 5. Questions and ratings during the workshop.

Question	CO	Simubone
First impression	8.3	8
Texture	6.6	7
Color	7	8.5
Milling spongy bone	7.6	8
Milling compact bone	7.6	8
Drilling spongy bone	8	5.5
Drilling compact bone	8.3	5.5
Gauging	6.6	6
Chip formation	6.3	6
Cup placement	8	7.5
Cup stability	8	9.5
Overall impression visually	8	8.5
Overall impression of the procedure	6.6	6
Usability for education	10	10
Average	*7.6*	*7.4*

4 3D file cleanup

The conversion of CT scan data into STL files for 3D printing and surgical planning represents a sophisticated and intricate process that may encounter various inaccuracies, particularly related to artifacts and processing errors. Such errors predominantly emerge during the segmentation phase, a crucial step in which the delineation between different tissue types is established to form a digital model of the intended anatomy. According to Gibson et al. (2021), the segmentation involves assigning specific Hounsfield unit values to distinguish between tissue types. The Hounsfield unit, a quantitative measure of radiodensity used in CT scans, is critical for this differentiation process (Hounsfield, 1973). However, the application of a singular threshold value for segmentation can oversimplify the complex nature of tissue densities, potentially leading to the exclusion of vital structures or the inclusion of extraneous elements in the resulting STL file. Moreover, the translation of a segmented CT dataset into an STL file entails the approximation of the anatomy's surface using triangular elements. While this step is essential for computational modeling, it introduces the possibility of faceting errors, as described by Ventola (2014). Such errors can compromise the smoothness of the anatomical representation, detracting from the model's fidelity to the actual biological structure.

In the context of producing bone-like structures for medical applications, this project has uncovered specific challenges associated with the STL files generated by the currently employed software. These challenges include numerous mesh holes, internal voids, and defects, as well as surfaces that are reversed or invalid. The labor-intensive process of rectifying these issues underscores the necessity for automating these corrections to streamline the preparation of 3D printable files, thereby enhancing the efficiency and practicality of this technology for surgical planning and implementation. Figure 6 show an example of errors (marked in red) in a mesh produced from a CT scan.

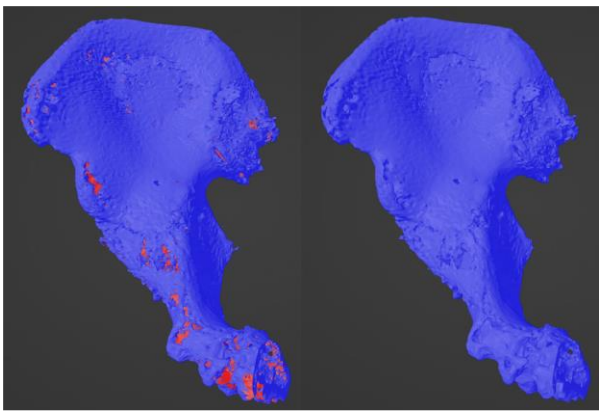

Figure 6. Geometry with internal holes and defects (left) compared to cleaned and fixed model (right).

In this project, we developed an automated approach within Blender to streamline various procedures, significantly enhancing the efficiency of mesh cleaning processes. The methodology incorporates a series of steps designed to refine and prepare the mesh for further use:

1. Remove Unlinked: This function identifies and eliminates vertices imported into Blender that are not integrated into the model's main structure. These disconnected points may be located either internally or externally relative to the model.
2. Mark Outer Geometry: Utilizing Blender's camera rotation feature, typically employed in rendering, this step generates multiple new vantage points surrounding the model. It then marks the geometry visible from each perspective. The accumulated markings from these diverse viewpoints collectively identify the entire model's external geometry.
3. Remove Inner Geometry: Following the comprehensive marking of the outer geometry, the selection is inverted to highlight the model's internal geometry instead. These marked internal structures are subsequently removed, streamlining the model's complexity.
4. Clean Up Mesh: This action replicates the initial step of removing unlinked components to address any additional disjointed geometry that may have emerged through the cleaning process. Subsequently, the Blender Remesh modifier is applied to reconstruct the mesh, effectively sealing any residual gaps.
5. Export Object as STL: The final step involves exporting the refined mesh as an STL file, making it ready for 3D printing or further digital manipulation.

This sequence of operations facilitates a thorough cleanup of 3D models where each step is implemented in a python script which can be run within Blender. A screenshot of the Blender interface supporting this process is presented in figure 7. The full python code which run in the background, together with a Blender file containing the scripts, can be found at GitHub (https://github.com/wiberganton/blender_mesh_cleanup).

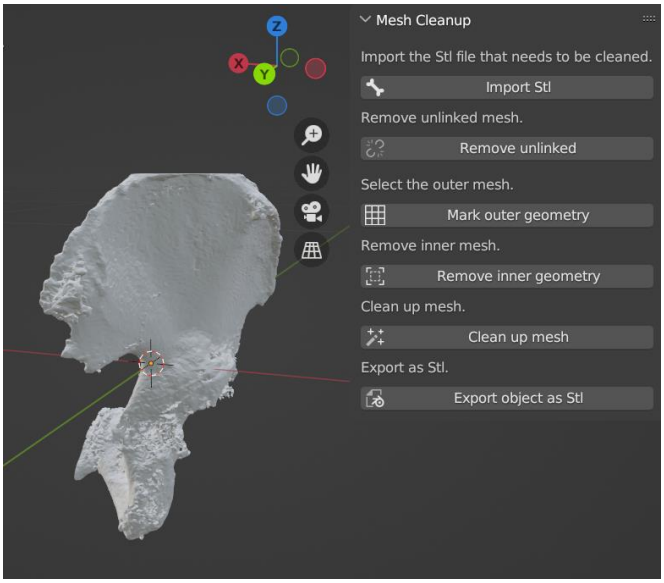

Figure 7. Screenshot from the Blender interface with one button for each of the steps in the procedure.

5 Results

The outcome of this research is an optimized process that transitions from an STL model, derived from a CT scan, to a 3D-printed bone structure designed for practicing orthopedic procedures. The comprehensive process is illustrated in figure 8. An efficient method for printing a hip bone from a CT scan for use in orthopedic training involves the use of an automated mesh cleaning technique, as detailed in Section 4. Utilizing the refined mesh, a standard FDM 3D printer is capable of fabricating bone-like structures. In this instance, the Anycubic Kobra 2 was employed to create the final model. The specific settings employed in the manufacturing process are outlined in Table 6. To mitigate the issue of cracking observed during experimental testing, a build orientation was chosen to be perpendicular to the milling direction in the hip cup. This approach is depicted in figure 9.

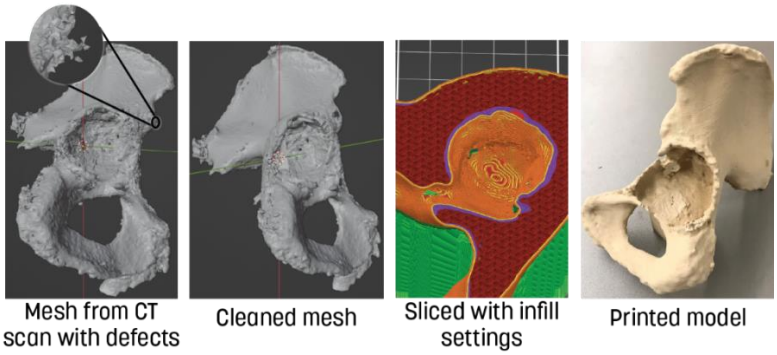

Figure 8. Showing the process from imported mesh to a printed model.

Table 6. 3D printing settings and material used.

Material	Infill type	Infill density	Nozzle size	Wall layers	Layer height
Clas Ohlsson Wood filament	Gyroid	30%	0.6 mm	2	0.3 mm

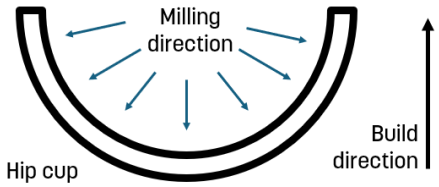

Figure 9. Build direction selected to avoid cracking between layers.

The printing duration and material expenses vary based on several factors, including the specific geometry employed, support strategies, among others. In this instance, the printing time amounted to 1366 minutes, and the total cost for materials, inclusive of the support structure, was 363 SEK (reflecting material prices as of July 2023)

6 Discussion and conclusion

The document provides a comprehensive examination of the integration of 3D printing technologies in the creation of anatomically accurate hip models for orthopedic training. The study highlights the process from CT scan acquisition through STL model preparation, focusing on automated mesh cleaning and optimal printing settings to produce bone-like structures. By addressing challenges such as material selection and layer orientation to prevent cracking, the research presents an advancement in medical training aids. The use of specific materials and printer settings, evaluated through extensive testing and expert feedback, underscores the potential of 3D printing in enhancing surgical training. The findings suggest that with careful consideration of printing parameters, 3D-printed models can closely mimic real bone characteristics, offering valuable tools for educational purposes and surgical preparation.

The initial assumptions regarding infill structure and material selection suggest there is room for broader exploration. Material tests were conducted with substitute tools, indicating that these results may not directly correlate with actual surgical procedures. Concerns were raised about polyurethane foam due to significant dust generation, which poses potential cleaning challenges and health risks from inhalation, despite its promising technical performance and tactile feedback. During material testing, both bone models experienced cracking along the layer direction, highlighting the inherent weakness of FDM-printed objects between layers, exacerbated when subjected to forces perpendicular to these layers during milling. However this could probably be counteracted by more investigation of the printer setup, either by having a more expensive printer, by adding an enclosure keeping a more stable temperature during the build, or by modifying the printer settings.

The workshop outcomes, influenced by participants' diverse skills and experiences, indicated the educational value of the produced bone models. Clas Ohlson’s wood filament and Simubone material displayed similar properties, with the former chosen for its cost-effectiveness (one third compared to Simubone) and availability in Sweden, despite Simubone's partial medical certification. The cost for the optimal bone model type was estimated at 363 SEK for a full print. This cost could be reduced through model optimizations and the use of alternative materials, including for support structures.

Finally, while the procedure shows promise for training and educational purposes, it has not been verified for medical treatment, highlighting the need for further validation to ensure its applicability in medical contexts.

References

Bardwell, T., 2023. FDM 3D Printing Miniatures Guide: Settings, Orientation & More. 3D sourced. URL https://www.3dsourced.com/guides/fdm-3d-printing-miniatures-guide/ (accessed 2.9.24).

Community, B.O., 2018. Blender - a 3D modelling and rendering package. Blender Foundation, Stichting Blender Foundation, Amsterdam.

Ćwik\la, G., Grabowik, C., Kalinowski, K., Paprocka, I., Ociepka, P., 2017. The influence of printing parameters on selected mechanical properties of FDM/FFF 3D-printed parts, in: IOP Conference Series: Materials Science and Engineering. IOP Publishing, p. 012033.

Davoudinejad, A., 2021. Vat photopolymerization methods in additive manufacturing, in: Additive Manufacturing. Elsevier, pp. 159–181.

D'Urso, P.S., Barker, T.M., Earwaker, W.J., Bruce, L.J., Atkinson, R.L., Lanigan, M.W., Arvier, J.F., Effeney, D.J., 1999. Stereolithographic biomodelling in cranio-maxillofacial surgery: a prospective trial. Journal of cranio-maxillofacial surgery 27, 30–37. https://doi.org/10/c2db9d

Gibson, I., Rosen, D., Stucker, B., Khorasani, M., 2021. Additive Manufacturing Technologies, 3rd ed. ed. Springer Nature, [S.l.].

Hoang, D., Perrault, D., Stevanovic, M., Ghiassi, A., 2016. Surgical applications of three-dimensional printing: a review of the current literature & how to get started. Annals of translational medicine 4. https://doi.org/10/f9nkzp

Hounsfield, G.N., 1973. Computerized transverse axial scanning (tomography): Part 1. Description of system. The British journal of radiology 46, 1016–1022. https://doi.org/10/bttqpg

Kazmer, D., 2017. Three-dimensional printing of plastics, in: Applied Plastics Engineering Handbook. Elsevier, pp. 617–634.

Liew, Y., Beveridge, E., Demetriades, A.K., Hughes, M.A., 2015. 3D printing of patient-specific anatomy: a tool to improve patient consent and enhance imaging interpretation by trainees. British Journal of Neurosurgery 29, 712–714. https://doi.org/10/gf2sk2

Marro, A., Bandukwala, T., Mak, W., 2016. Three-dimensional printing and medical imaging: a review of the methods and applications. Current problems in diagnostic radiology 45, 2–9. https://doi.org/10/gmwf78

Michalski, M.H., Ross, J.S., 2014. The shape of things to come: 3D printing in medicine. Jama 312, 2213–2214. https://doi.org/10/gtg8wc

Nefronus, 2023. Simple bone.

O'Connell, J., 2018. The Types of FDM 3D Printers (Cartesian, CoreXY, & More). All3DP. Retrieved June 9, 2022.

Reilly, G.C., Currey, J.D., 1999. The development of microcracking and failure in bone depends on the loading mode to which it is adapted. Journal of Experimental Biology 202, 543–552. https://doi.org/10/gtg8wb

Rengier, F., Mehndiratta, A., Von Tengg-Kobligk, H., Zechmann, C.M., Unterhinninghofen, R., Kauczor, H.-U., Giesel, F.L., 2010. 3D printing based on imaging data: review of medical applications. International journal of computer assisted radiology and surgery 5, 335–341. https://doi.org/10/ft5xdm

Rho, J.-Y., Kuhn-Spearing, L., Zioupos, P., 1998. Mechanical properties and the hierarchical structure of bone. Medical engineering & physics 20, 92–102. https://doi.org/10/bcmxvs

Robling, A.G., Castillo, A.B., Turner, C.H., 2006. Biomechanical and molecular regulation of bone remodeling. Annu. Rev. Biomed. Eng. 8, 455–498. https://doi.org/10/cbxd3g

Saladin, K.S., Porth, C., 2010. Anatomy & physiology: the unity of form and function. McGraw-Hill New York.

Soames, R.W., Palastanga, N., 2018. Anatomy and Human Movement E-Book: Structure and function. Elsevier Health Sciences.

Treatstock, n.d. Express guide of FDM printing materials. URL https://www.treatstock.com/guide/article/118-express-guide-of-fdm-3d-printing-materials (accessed 2.9.24).

Ventola, C.L., 2014. Medical applications for 3D printing: current and projected uses. Pharmacy and Therapeutics 39, 704.

Contact: Anton Wiberg, Linköping University, anton.wiberg@liu.se